YMTHE, Volume *31*

Supplemental Information

WNT-modulating gene silencers as a gene therapy for osteoporosis, bone fracture, and critical-sized bone defects

Won-Taek Oh, Yeon-Suk Yang, Jun Xie, Hong Ma, Jung-Min Kim, Kwang-Hwan Park, Daniel S. Oh, Kyung-Hyun Park-Min, Matthew B. Greenblatt, Guangping Gao, and Jae-Hyuck Shim

Supplementary Materials for:

WNT-modulating gene silencers as a gene therapy for osteoporosis, bone fracture, and critical-sized bone defects

Won-Taek Oh[1,2]†, Yeon-Suk Yang[1]†, Jun Xie[3,4,5], Hong Ma[3,4,5], Jung-Min Kim[1], Kwang-Hwan Park[2], Daniel S. Oh[6], Kyung-Hyun Park-Min[7,8], Matthew B. Greenblatt[8,9], Guangping Gao[3,4,5,10]*, and Jae-Hyuck Shim[1,3,10]*

†These authors contributed equally to this work.

*Corresponding authors: Jae-Hyuck Shim. Email: jaehyuck.shim@umassmed.edu and Guangping Gao. Email: guangping.gao@umassmed.edu

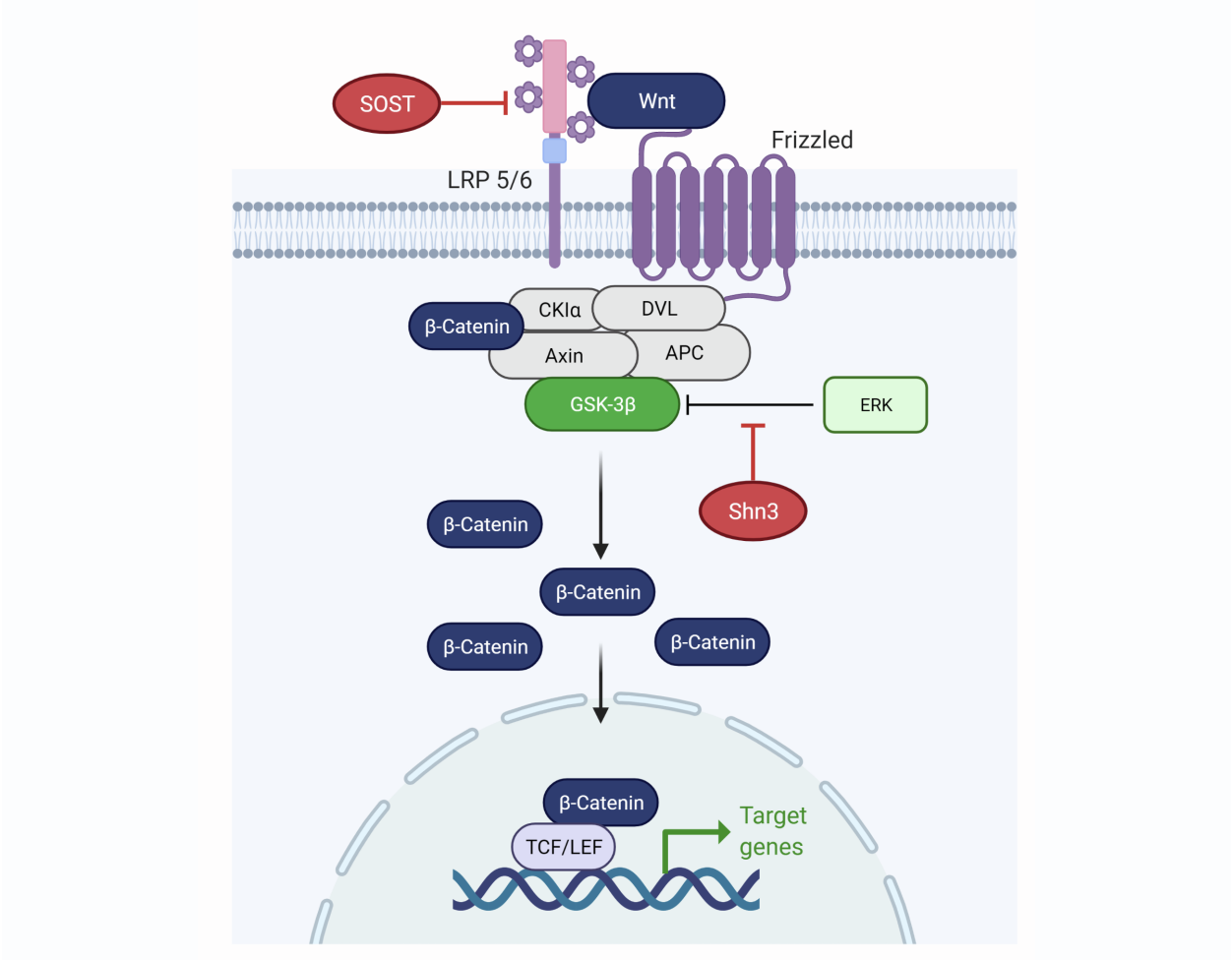

Fig. S1. Schematic diagram showing the molecular mechanism of SHN3 and SOST in the WNT/β-catenin pathway (created with biorender.com). Abbreviations: CK1α, casein kinase 1α; LRP 5/6, low-density lipoprotein receptor-related proteins 5 and 6; DVL, dishevelled; APC, adenomatous polyposis coli; GSK-3β, glycogen synthase kinase 3 beta; ERK, extracellular signal-regulated kinase; TCF/LEF, T-cell factor/lymphoid enhancer factor.

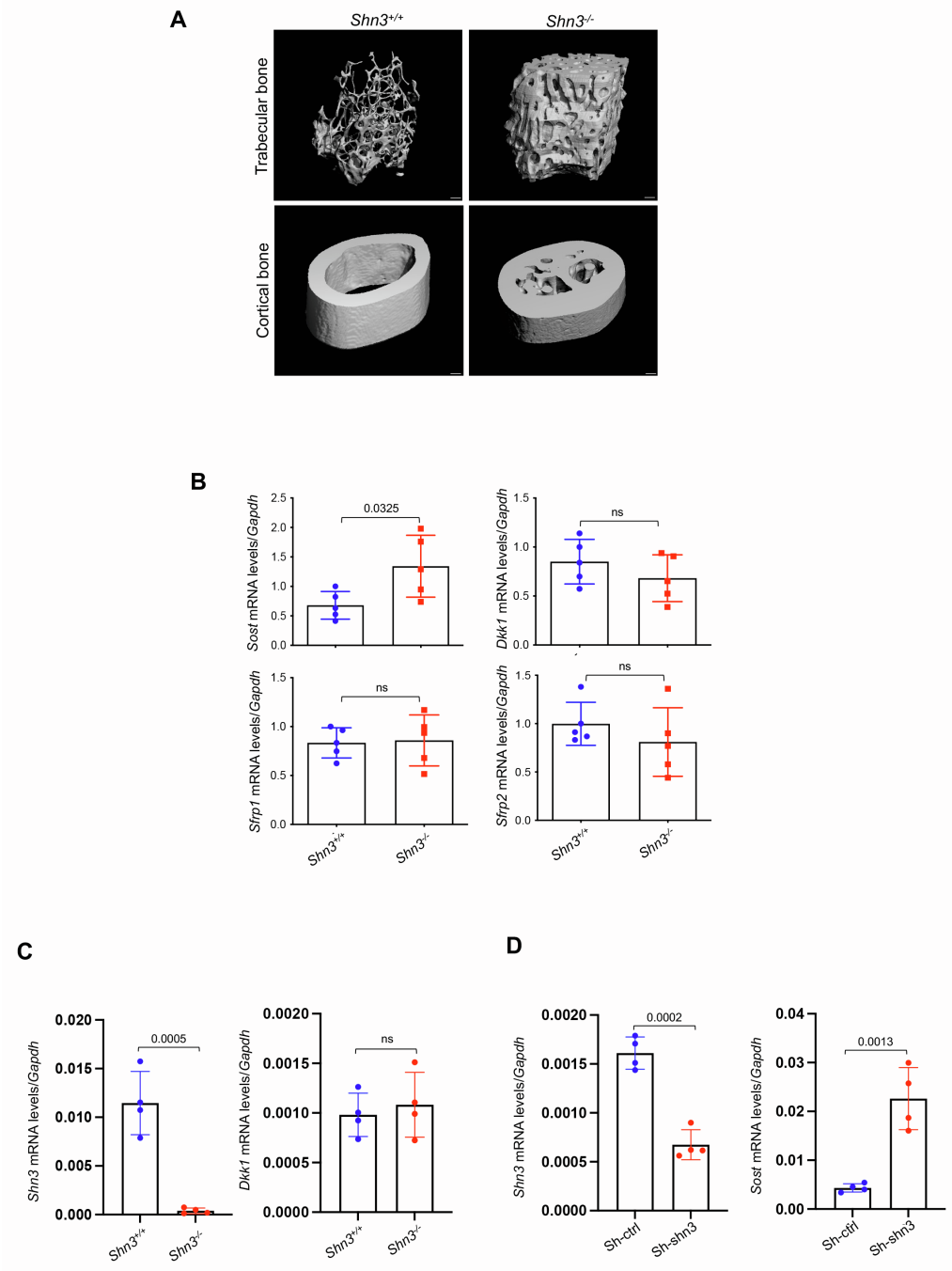

Fig. S2. Expression of secreted WNT antagonists in *Shn3*$^{-/-}$ mice.
A. MicroCT analysis showing trabecular bone mass and midshaft cortical bone thickness in femurs obtained from 2-month-old *shn3*$^{+/+}$ and *shn3*$^{-/-}$ mice. Scale bar: 200 μm. **B.** mRNA levels of secreted WNT antagonists in the tibia, *Sost, Dkk1, Sfrp1, or Sfrp2,* were measured by RT-PCR. **C.** Calvarial osteoblasts were isolated from *shn3*$^{+/+}$ and *shn3*$^{-/-}$ pups at postnatal day 4 and mRNA levels of *Dkk1* were measured by RT-PCR. **D.** The osteocyte line OCY454 was transduced with lentiviruses expressing control-shRNA (Sh-ctrl)- or Shn3-shRNA (Sh-shn3) and mRNA levels of *Sost* were measured by RT-PCR. Values represent mean ± SD by an unpaired two-tailed Student's t-test. ns, not significant.

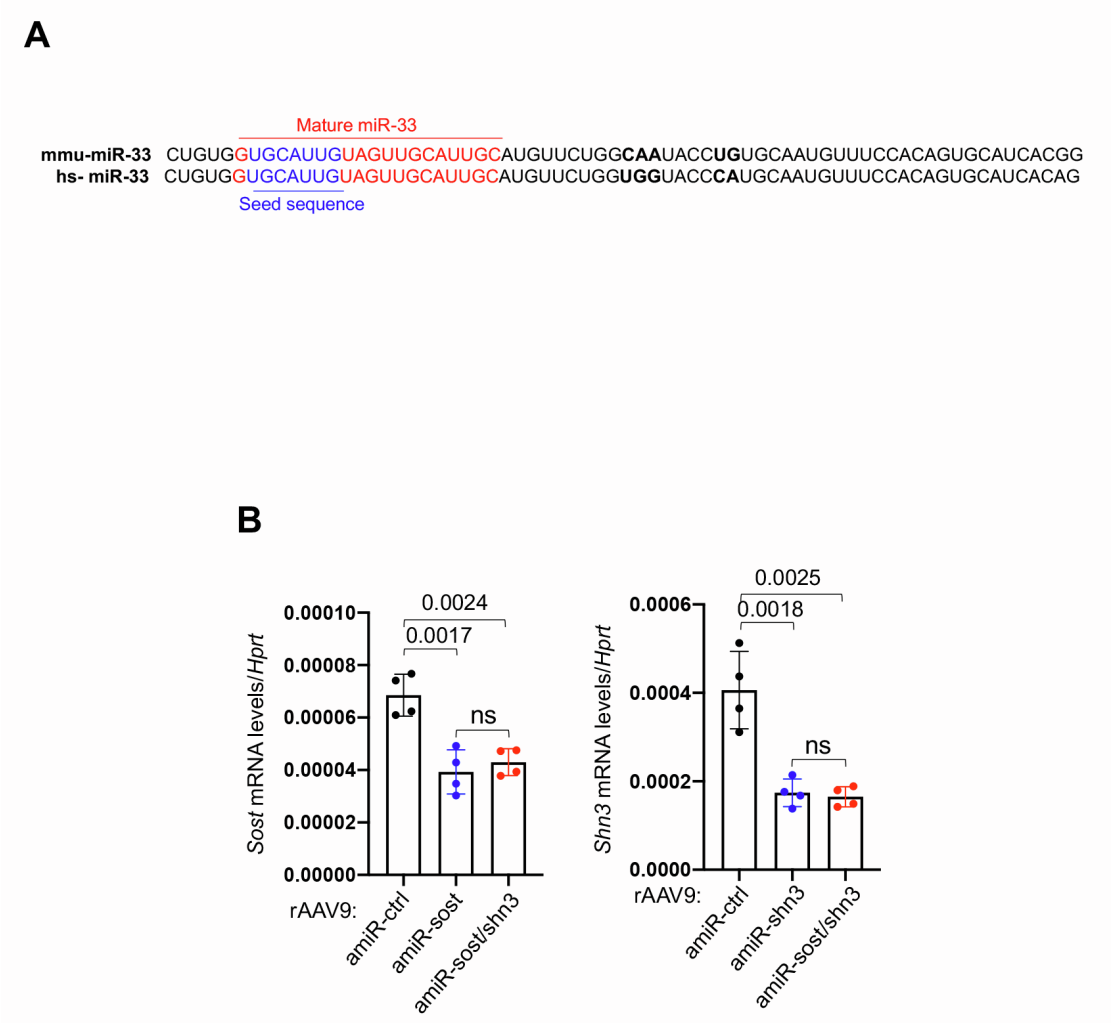

Fig. S3. Characterization of human amiR targeting mouse *Shn3*.
A. Nucleotide sequences of mouse (mmu-miR-33) and human (hs-miR-33) miR-33 that include mature and seed sequences (in blue) of miR-33. **B.** The Ocy454 osteocytic cell line was incubated with rAAV9.DSS carrying *amiR-ctrl*, *amiR-shn3*, *amiR-sost*, or *amiR-shn3/sost*, cultured under differentiation conditions for six days, and *Shn3* and *Sost* mRNA levels were measured by RT-PCR. Values represent mean ± SD by a one-way ANOVA test. ns, not significant.

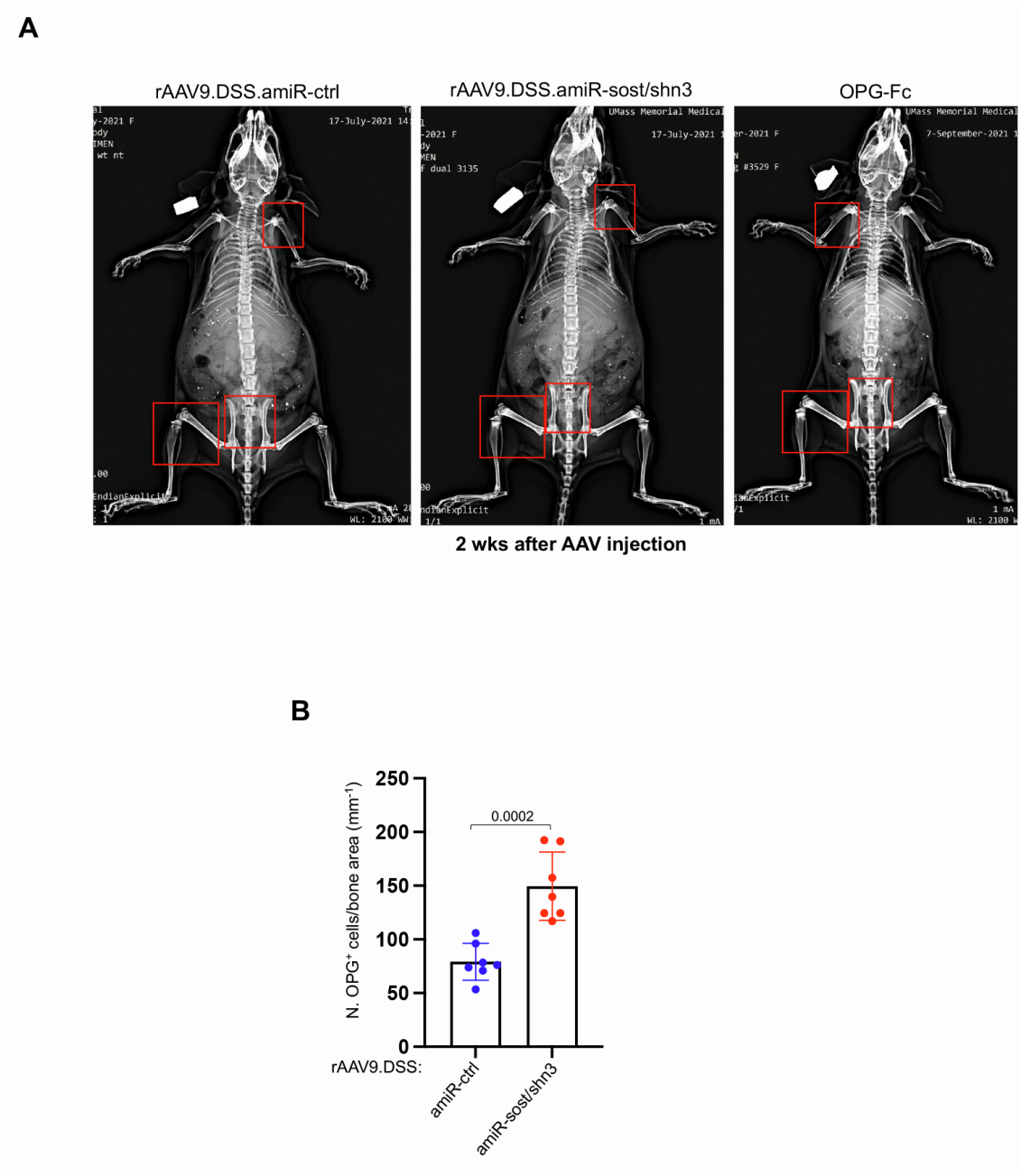

Fig. S4. Systemic delivery of WNT-modulating gene silencers increases bone accrual. **A.** One-month-old mice were treated with a single dose of rAAV9.DSS vectors carrying *amiR-ctrl* or *amiR-shn3/sost* (5 x 10^{13} vg/kg) via intravenous (i.v.) injection or with OPG-Fc (1 mg/kg) via intraperitoneal (i.p.) injection and two weeks later, bone accrual was assessed by radiography. Red boxes indicate the areas of increased bone accrual. The same experiment was performed in **Fig. 2B**. **B.** Two-month-old mice were injected i.v. with rAAV9.DSS (5 x 10^{13} vg/kg) carrying *amiR-ctrl* or *amiR-sost/shn3*, and four weeks later, immunohistochemistry for OPG was performed in AAV-treated femurs and OPG-expressing cells were quantitated (n = 7). The same experiment was performed in **Fig. 2I**. Values represent mean ± SD by a one-way ANOVA test.

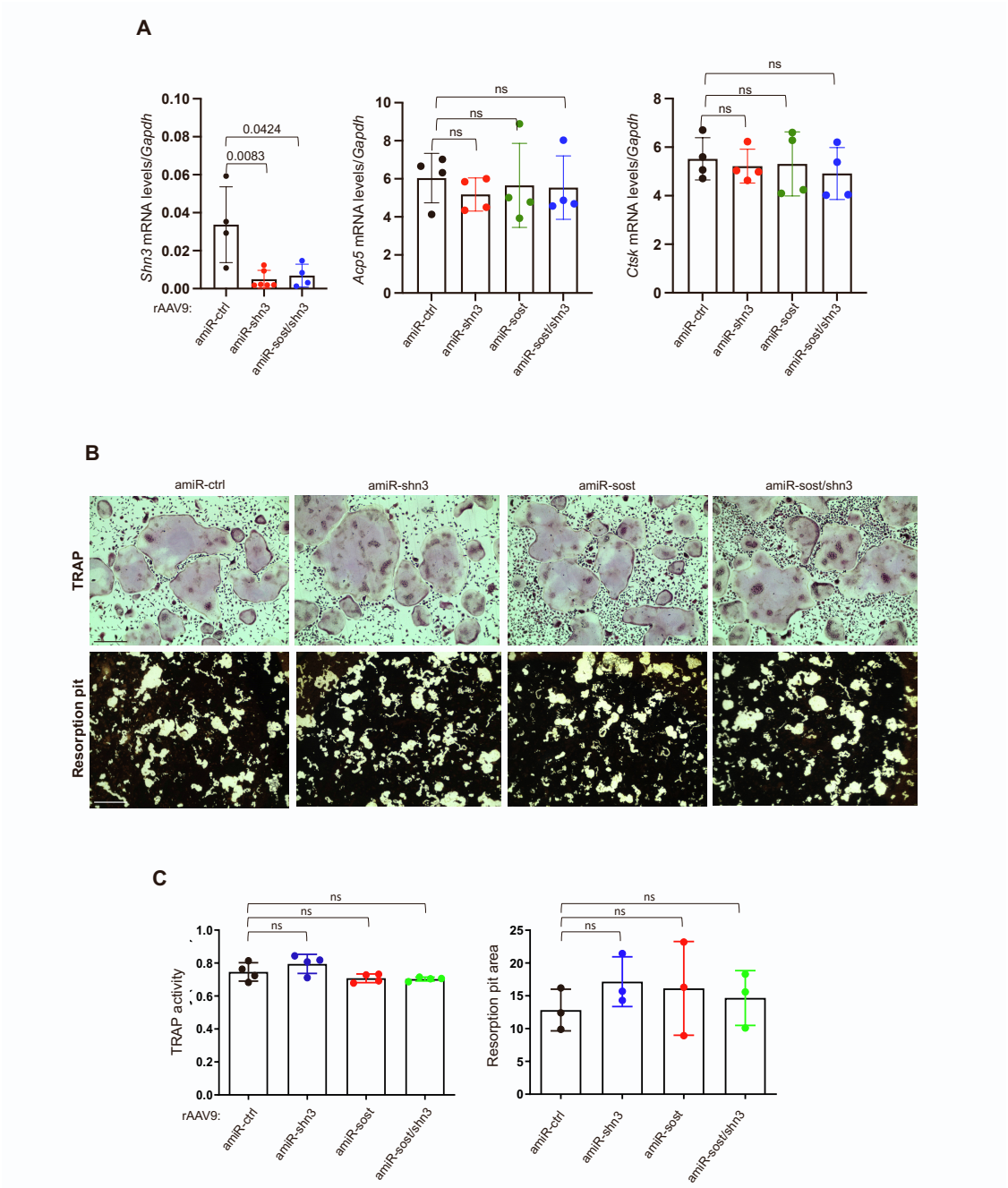

Fig. S5. Effects of WNT-modulating gene silencers on osteoclast differentiation *in vitro*. Bone marrow-derived monocytes (BMMs) harvested from 2-month-old mice were treated with M-CSF (20 ng/ml) and RANKL (10 ng/ml) for one day and then transduced with rAAV9.DSS carrying *amiR-ctrl*, *amiR-shn3*, *amiR-sost*, or *amiR-shn3/sost* (5 x 10^6 MOI). AAV-transduced BMMs were cultured with M-CSF and RANKL for six days to differentiate them into mature osteoclasts. **A.** Expression of *Shn3* and osteoclastogenic genes, *Acp5* and *Ctsk*, was assessed by RT-PCR and normalized to *Gapdh* (n = 4). *Sost* mRNAs were not detected by RT-PCR. **B, C.** Osteoclast differentiation and resorption activity were assessed by TRAP staining and resorption pit assay, respectively (n = 4). Scale bars: 1 mm. Values represent mean ± SD by a one-way ANOVA test. ns, not significant.

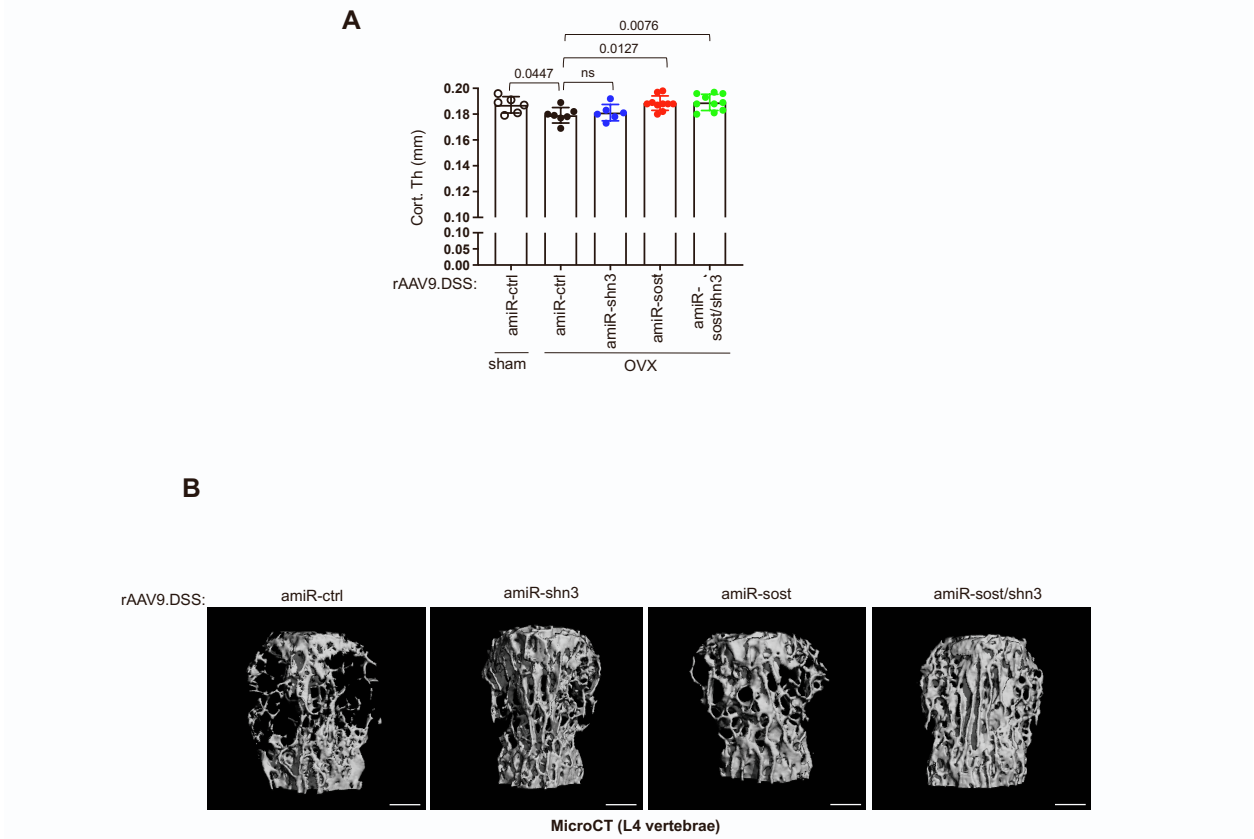

Fig. S6. Bone-targeted AAV gene silencers reverse bone loss in mouse models of osteoporosis. **A.** Sham or OVX surgery was performed on three-month-old female mice, and six weeks later, mice were injected i.v. with rAAV9.DSS (5 x 10^{13} vg/kg) carrying *amiR-ctrl*, *amiR-shn3, amiR-sost,* or *amiR-sost/shn3*. Eight weeks later, cortical thickness of AAV-treated femurs was assessed by microCT (n = 5–10). The same experiment was performed in **Fig. 3E**. **B.** 20-month-old male mice were injected i.v. with rAAV9.DSS (5 x 10^{13} vg/kg) carrying *amiR-ctrl*, *amiR-shn3, amiR-sost, or amiR-sost/shn3*, and two months later, trabecular bone mass in lumbar vertebrae (L4) was assessed by microCT. Representative 3D-reconstruction is displayed (n = 8–10). Scale bars: 500 µm. The same experiment was performed in **Fig. 3I**. Scale bars: 1 mm. Values represent mean ± SD by a one-way ANOVA test. ns, not significant.

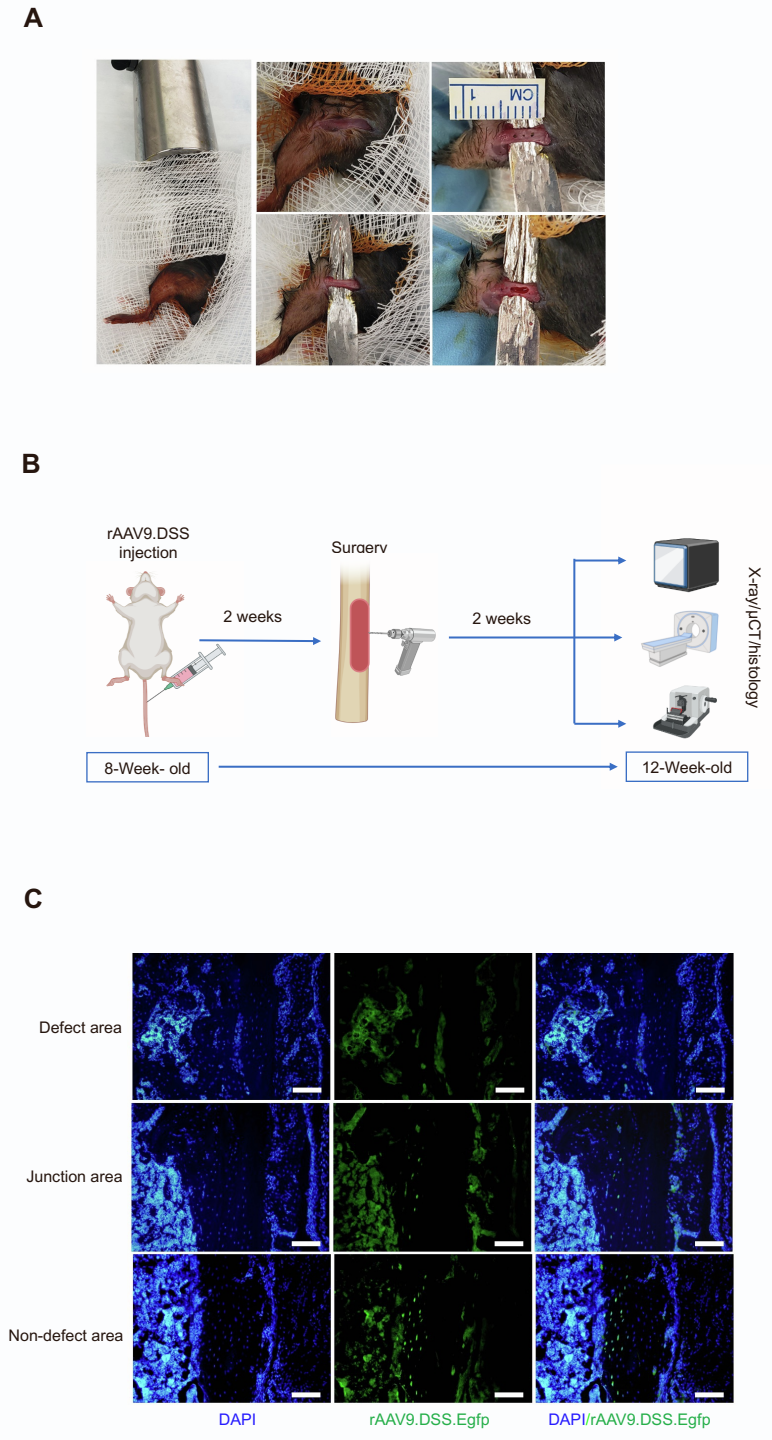

Fig. S7. Effects of WNT-modulating gene silencers on the healing of cortical bone defects. **A.** Images showing the surgical procedure of cortical bone defect in the femur. **B.** Diagram of the study and treatment methods (created with biorender.com). **C.** 8-week-old mice were i.v. injected with rAAV9.DSS.egfp (5 x 10^{13} vg/kg), and two weeks later, a 3 mm-length of cortical bone defect was generated on the lateral aspect of the left femurs. GFP expression in the cryo-sectioned femurs was visualized by fluorescence microscopy two weeks post-surgery (n=3). Scale bars: 500 μm. The same experiment was performed in **Fig. 4A**.

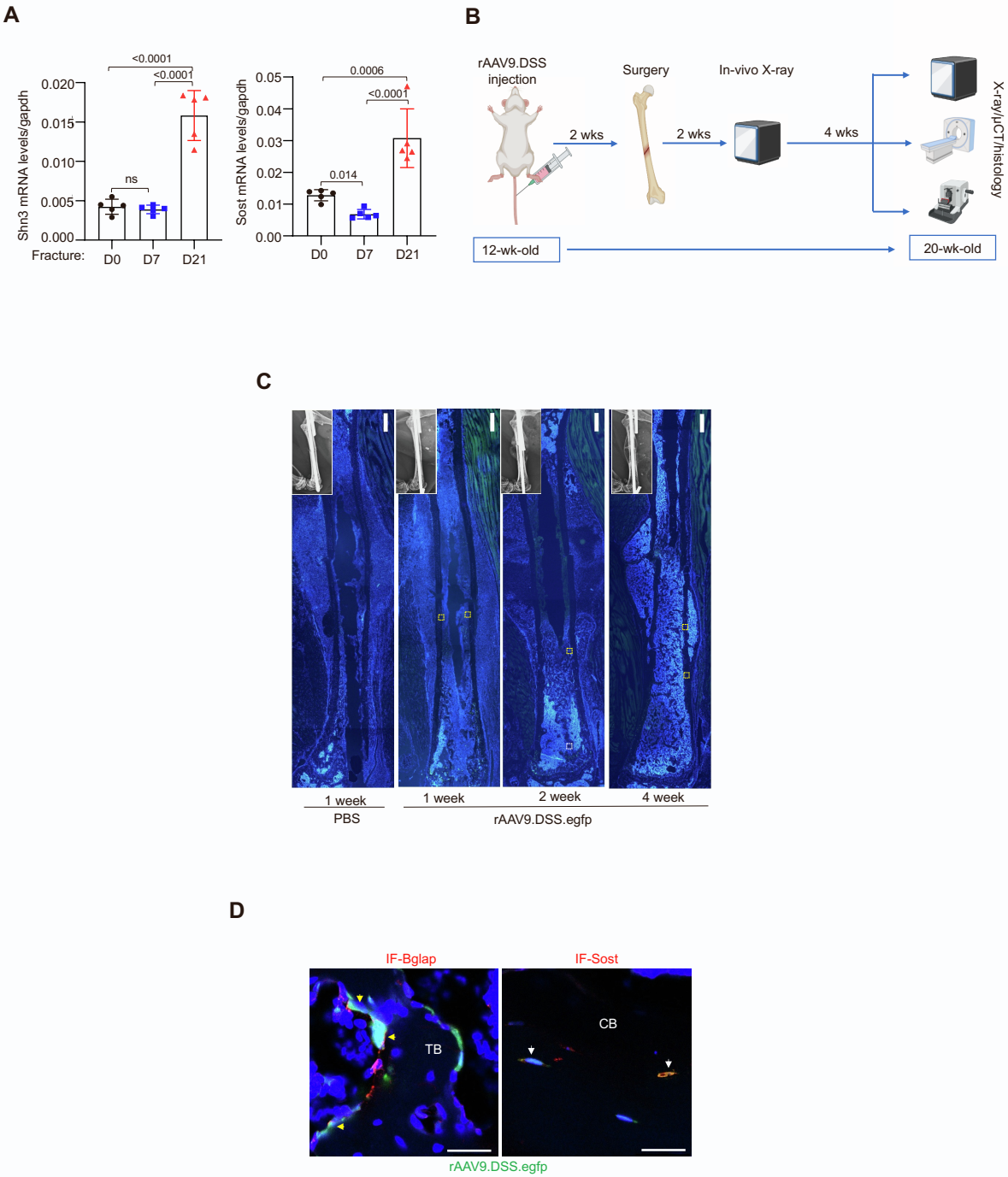
A
<0.0001
<0.0001
ns
Shn3 mRNA levels/gapdh
0.020
0.015
0.010
0.005
0.000
Fracture:
D0
D7
D21
0.0006
<0.0001
0.014
Sost mRNA levels/gapdh
0.05
0.04
0.03
0.02
0.01
0.00
D0
D7
D21
B
rAAV9.DSS injection
2 wks
Surgery
2 wks
In-vivo X-ray
4 wks
X-ray/μCT/histology
12-wk-old
20-wk-old
C
1 week
PBS
1 week
2 week
4 week
rAAV9.DSS.egfp
D
IF-Bglap
IF-Sost
TB
CB
rAAV9.DSS.egfp

Fig. S8. Systemic delivery of a bone-targeted AAV can transduce osteoblast-lineage cells at fracture sites.

A. Tissue RNA was harvested from the tibial fracture sites, and mRNA levels of *Shn3* and *Sost* were measured by RT-PCR (n=5/group). **B.** Diagram of the study and treatment methods (created with biorender.com). **C-D.** Three-month-old mice were i.v. injected with rAAV9.DSS.egfp, and two weeks later, femoral osteotomy and intramedullary fixation were performed on the left femurs. To visualize AAV-transduced cells in the fracture areas, EGFP expression in the cryo-sectioned femurs was assessed by fluorescence microscopy 1, 2, and 4 weeks postoperatively (n = 3, **C**). Alternatively, cryo-sectioned femurs were immunostained with Bglap (osteoblasts, yellow arrows) or Sost (Osteocytes, white arrows, **D**). The same experiment was performed in **Fig. 4E.** Scale bars: C, 600 μm; D, 25 μm. Values represent mean ± SD. Significance was tested with a one-way ANOVA test. ns, not significant.

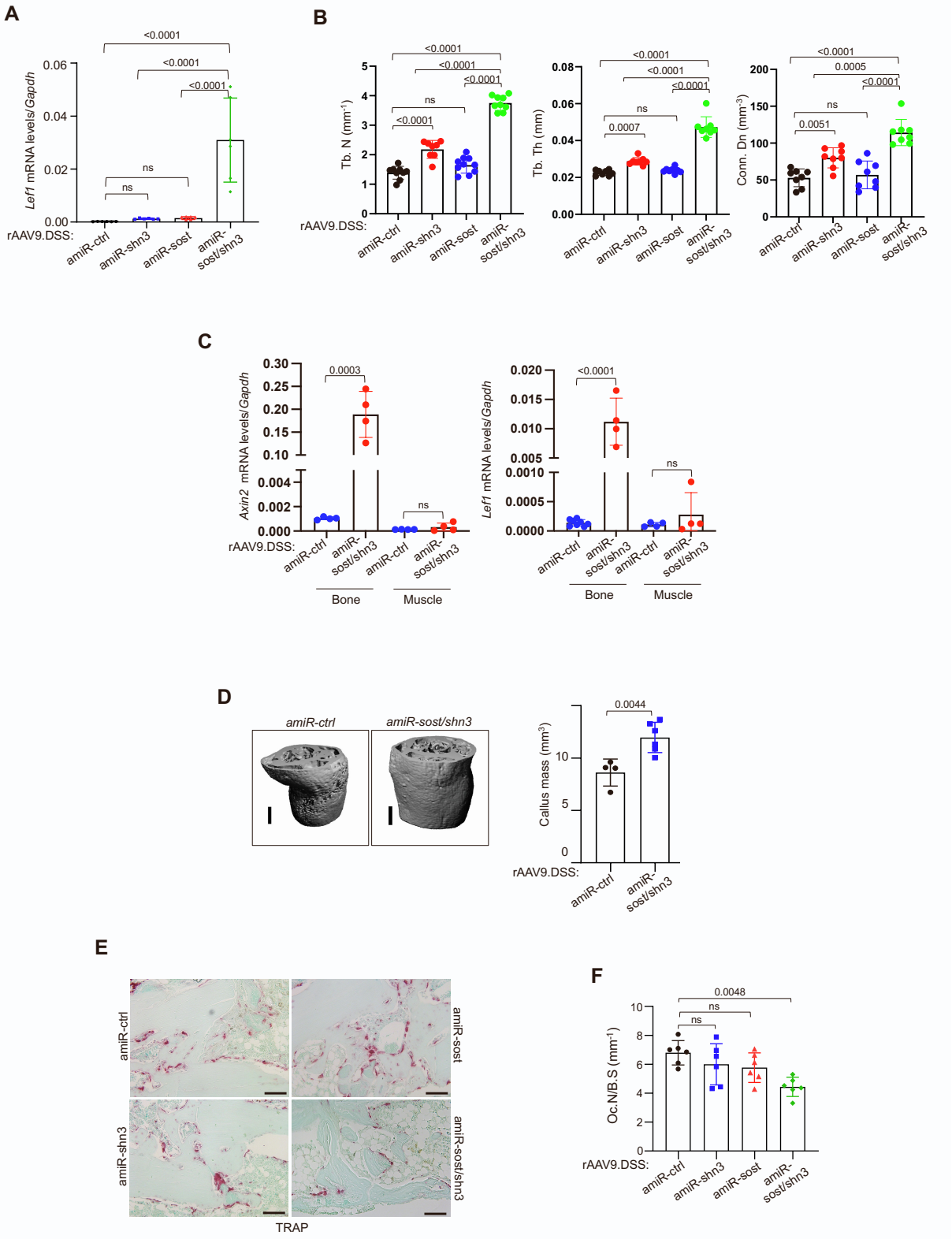
A
Lef1 mRNA levels/Gapdh
<0.0001
<0.0001
<0.0001
ns
ns
rAAV9.DSS:
amiR-ctrl
amiR-shn3
amiR-sost
amiR-sost/shn3
B
Tb. N (mm-1)
Tb. Th (mm)
Conn. Dn (mm-3)
0.0007
0.0005
0.0051
C
Axin2 mRNA levels/Gapdh
Lef1 mRNA levels/Gapdh
0.0003
Bone
Muscle
D
amiR-ctrl
amiR-sost/shn3
Callus mass (mm3)
0.0044
E
TRAP
F
Oc.N/B.S (mm-1)
0.0048

Fig. S9. Effects of WNT-modulating gene silencers on bone fracture healing.
Three-month-old mice were i.v. injected with rAAV9.DSS carrying *amiR-ctrl*, *amiR-shn3, amiR-sost,* or *amiR-sost/shn3*, and two weeks later, femoral osteotomy and intramedullary fixation were performed on the left femurs. mRNA levels of the β-catenin target gene *Lef1* in RNA from the contralateral tibia **(A)** or the skeletal muscle of the fractured femurs **(C)** were measured six weeks post-fracture (n = 8). The same experiment was performed in **Fig. 4G,** but for Axin2 mRNA. Trabecular bone mass of contralateral femurs without the surgery (**B)** and callus bone mass in the fractured sites (**D)** were assessed by microCT (n = 8). Fractured sites of AAV-treated femurs were stained for TRAP and TRAP-stained osteoclasts were quantitated (n =6, **E, F**). Tb.N: trabecular bone number, Tb.Th: trabecular bone thickness, Conn.D: connective density. Oc.N/B.S: osteoclast number/bone surface. Scale bar: D, 1 mm; E, 100 μm. Values represent mean ± SD by a one-way ANOVA test. ns, not significant.

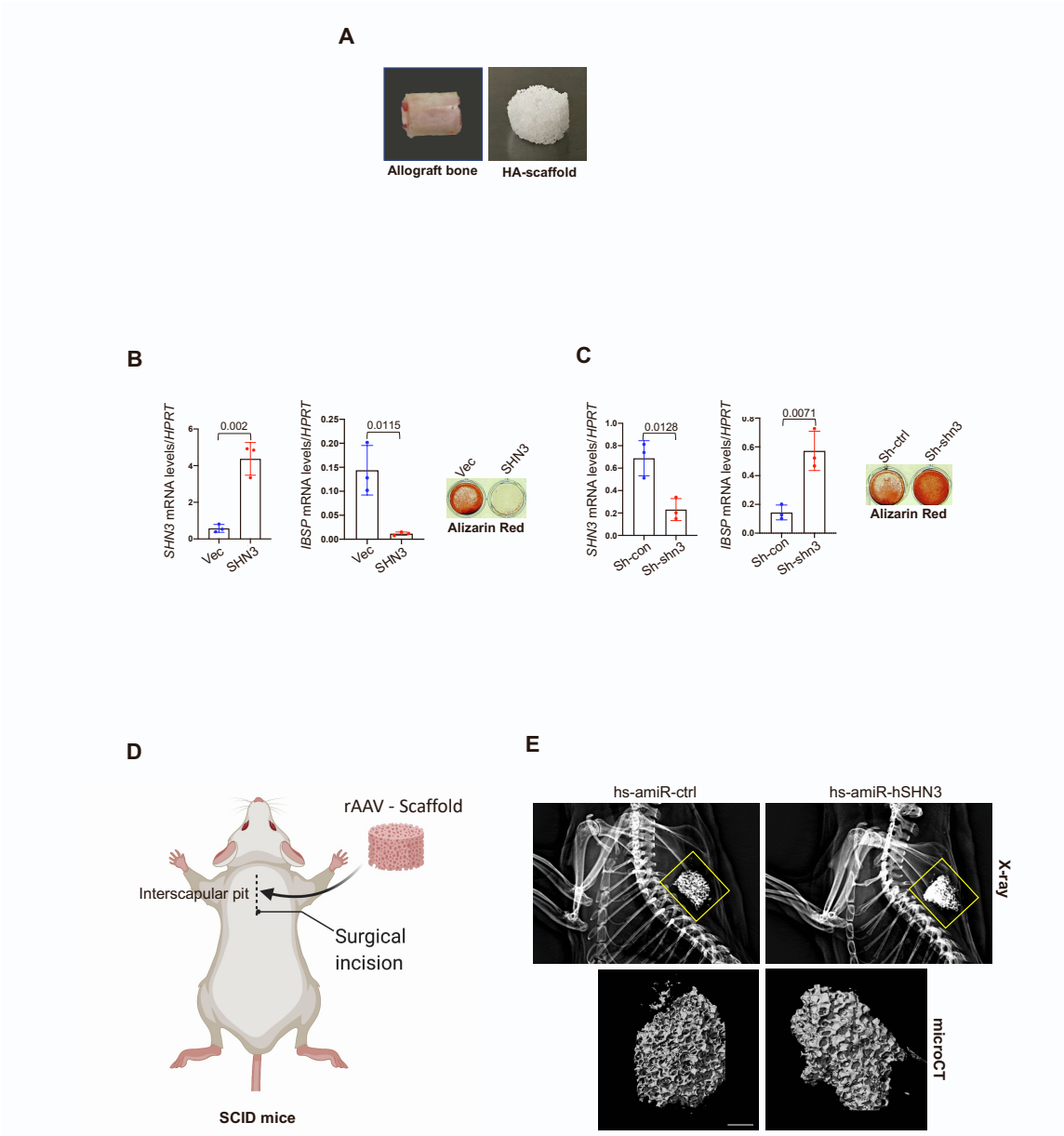

Fig. S10. Generation of a human skeletal organoid in xenograft mice.
A. Representative pictures showing mouse decellularized bone graft and hydroxyapatite (HA)-based scaffold. **B, C.** Human BMSCs were transduced with lentiviruses expressing vector control (Vec), mouse SHN3 (1-3557 aa, **B**), control-shRNA (Sh-con), or Shn3-shRNA (Sh-shn3, **C**), cultured under osteogenic conditions, and mRNA levels of *SHN3* and *IBSP* were measured by RT-PCR. Alternatively, mineralization deposit was assessed by alizarin red staining (n=3). **D, E.** Diagram showing a surgery procedure to implant a human skeletal organoid into the interscapular fat pad of immunodeficient SCID mice (created with biorender.com) **(D)**. The HA-scaffold was incubated with rAAV9.DSS carrying *hs-amiR-ctrl or hs-amiR-hSHN3* for one hour, and then human BMSCs were cultured on the AAV-treated scaffold under osteogenic conditions for two days. The treated scaffold was implanted into the interscapular fat pads, and four weeks later, bone formation was assessed by radiography **(E, top)** and microCT (**E, bottom**, n=5). Values represent mean ± SD by an unpaired two-tailed Student's t-test.

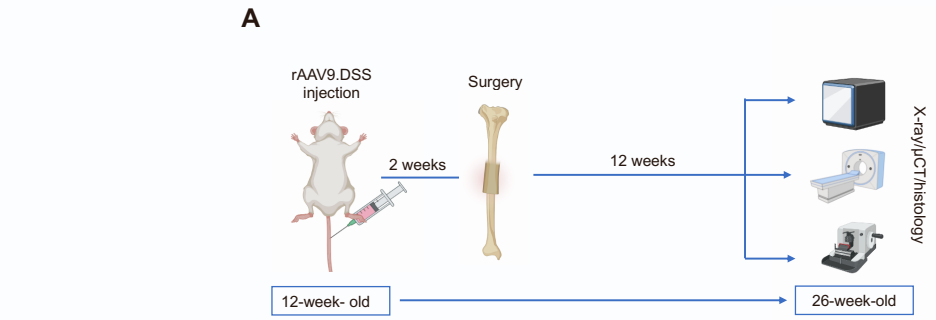
A
rAAV9.DSS injection
Surgery
2 weeks
12 weeks
X-ray/μCT/histology
12-week- old
26-week-old

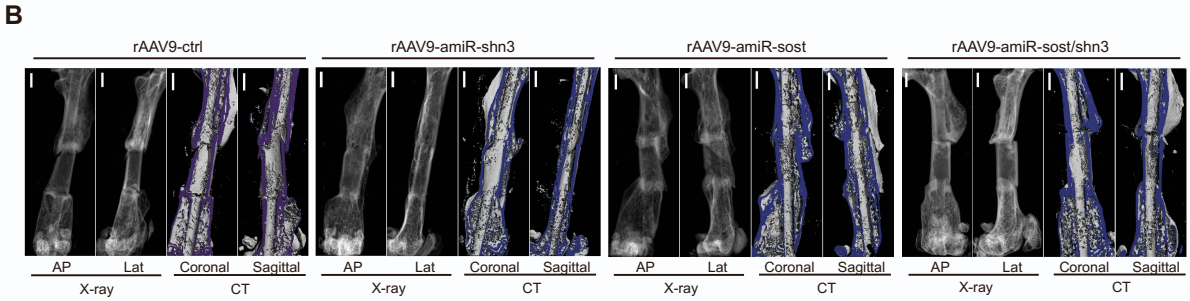
B
rAAV9-ctrl
rAAV9-amiR-shn3
rAAV9-amiR-sost
rAAV9-amiR-sost/shn3
AP
Lat
Coronal
Sagittal
X-ray
CT

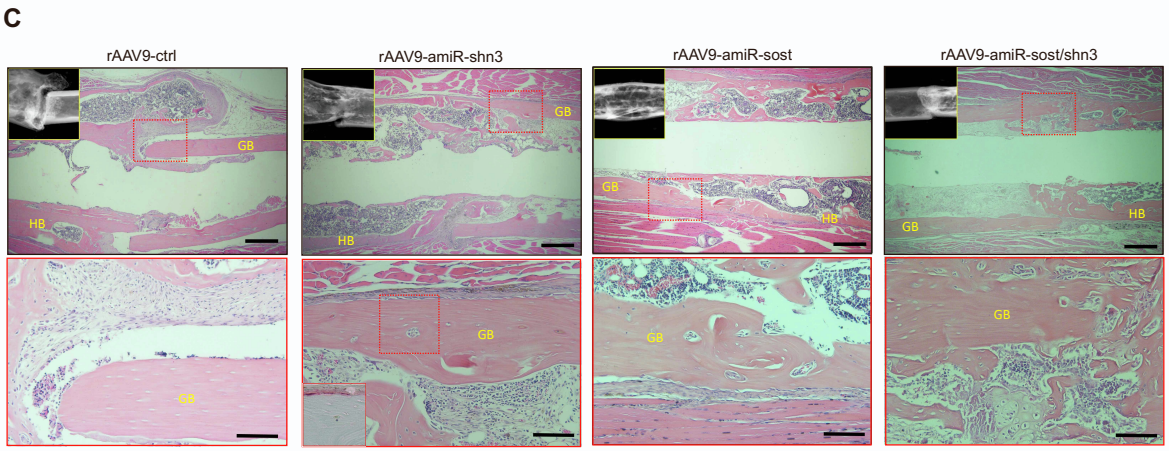
C
rAAV9-ctrl
rAAV9-amiR-shn3
rAAV9-amiR-sost
rAAV9-amiR-sost/shn3
GB
HB

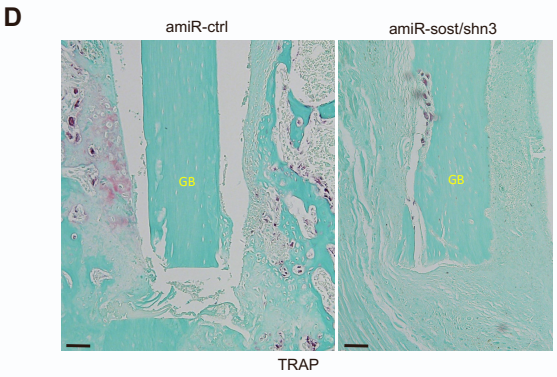
D
amiR-ctrl
amiR-sost/shn3
GB
TRAP

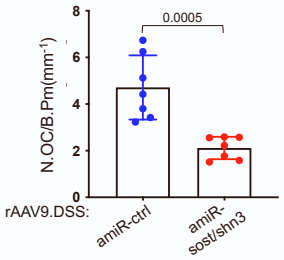
E
0.0005
N.OC/B.Pm(mm-1)
8
6
4
2
0
rAAV9.DSS:
amiR-ctrl
amiR-sost/shn3

Fig. S11. Therapeutic effects of systemically delivered WNT-modulating gene silencers on critical-sized bone defect

A. Diagram of the study and treatment methods (created with biorender.com). **B-E.** Three-month-old mice were i.v. injected with rAAV9.DSS (5 x 10^{13} vg/kg) carrying *amiR-ctrl, amiR-shn3*, *amiR-sost,* or *amiR-sost/shn3*, and two weeks later, decellularized isograft was implanted into the osteotomy site of the left femurs. Twelve weeks later, radiography, microCT, and H&E staining were performed on the injured femurs to assess the rate of osseous union between the implanted isograft to the host bone. (n = 5–6, **B, C**). HB: host bone, GB: graft bone. The same experiment was performed in **Fig. 6A and B**. Alternatively, the injured femurs were stained for TRAP and TRAP-stained osteoclasts were quantitated (n = 7, **D, E**). Scale bars: B, 1 mm; C, top, 400 μm; C bottom, D, 100 μm. Values represent mean ± SD by an unpaired two-tailed Student's t-test.

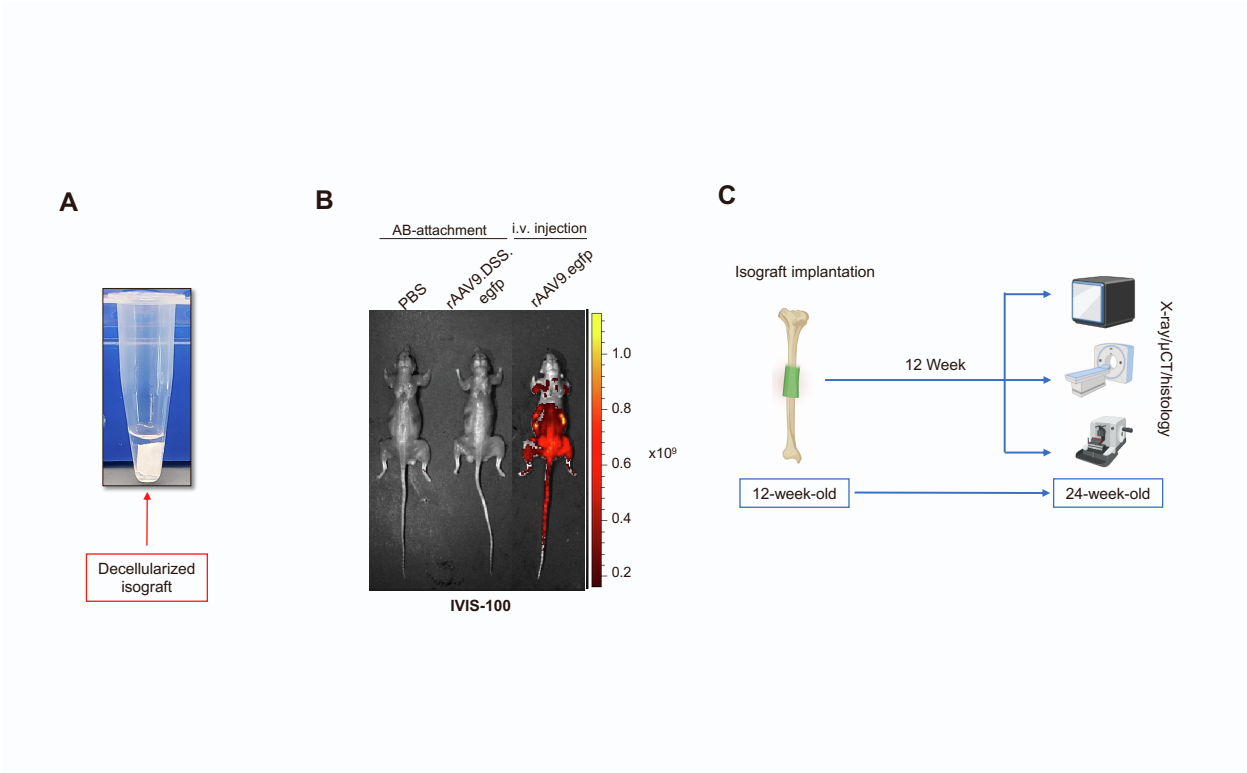

Fig. S12. Transplantation of the isograft carrying WNT-modulating gene silencers to the osteotomy sites in a mouse model of critical-sized bone defect

A. Preparation of decellularized isograft attached with rAAV9.DSS. Decellularized isograft was incubated with rAAV9.DSS (2.5 x 10^{11} GC) for one hour. **B.** PBS-treated or rAAV9.DSS.*egfp*-attached isograft was implanted into the osteotomy site of left femurs in 3-month-old mice, and three weeks later, EGFP expression in whole body was monitored by IVIS-100 optical imaging. For systemic delivery, rAAV9.DSS.*egfp* (5 x 10^{13} vg/kg) was i.v. injected into mice (n = 3). The same experiment was performed in **Fig. 6C**. **C.** Diagram of the study and treatment methods (created with biorender.com).

Tables S1-S2

Table S1

	amiR-ctrl	amiR-shn3	amiR-sost	amiR-shn3/sost
WNT signaling threshold	weak	intermediate	intermediate	strong
Osteogenesis	no effect	mild increase	mild increase	strong increase and wane over time
Osteoclastogenesis	no effect	no effect	mild decrease	strong decrease by OPG
Bone accrual	no effect	mild increase	mild increase	strong increase
Early bone regeneration	no effect	increase	increase	increase
Osteoporosis	no effect	complete reversal	partial reversal	complete reversal
Bone fracture healing	no effect	increase	increase	little to mild increase
Critical-sized bone defect healing	no effect	increase	increase	no effect

Table S2

Gene	Forward	Reverse
Human *Shn3*	GCCCTATGTGTGCAAGCACTGT	AGTCCTGGAACAGGTCGTCACT
Mouse *Shn3*	AGAGGCCATTCAGACGAGTGT	CTGCGGAAGCTGAGAGATGT
Mouse *Gapdh*	ACTGAGCAAGAGAGGCCCTA	TATGGGGGTCTGGGATGGAA
Mouse *Actb*	AGGGAAATCGTGCGTGACAT	GAACCGCTCGTTGCCAATAG
Mouse *Lef1*	CCAAGCAAGGCATGTCCAGACACC	GCCTGACAGTGAGGATGGGTAGGG
Mouse *Dkk1*	ATCTGTCTGGCTTGCCGAAAGC	GAGGAAAATGGCTGTGGTCAGAG
Human *BGLAP*	AGAGTCCAGCAAAGGTGCAG	TCAGCCAACTCGTCACAGTC
Human *IBSP*	CAACAGCACAGAGGCAGAAA	TTGTGGTGGGGTTGTAGGTT
Mouse *Axin2*	GCAGATGAACCTGAAGGATACC	TTGATGCCATCTCGTATGTAGG
Mouse *Sost*	CTTCAGGAATGATGCCACAGAGGT	ATCTTTGGCGTCATAGGGATGGTG
Mouse *Hprt*	CTGGTGAAAAGGACCTCTCGAAG	CCAGTTTCACTAATGACACAAACG
Human *HPRT*	GCTATAAATTCTTTGCTGACCTGCTG	AATTACTTTTATGTCCCCTGTTGACTGG
EGFP	AGCAAAGACCCCAACGAGAA	GGCGGCGGTCACGAA
EGFP-probe	6FAM-CGCGATCACATGGTCCTGCTGG-TAMRA	
$(AspSerSer)_6$	GATTCATCAGATTCTTCTGATTCATCCGACTCTTCTGACAGTTCAGACAGCTCT	
$(Asp)_{14}$	GATGATGATGATGATGATGATGATGATGATGATGATGAT	
amiR-33-ctrl (*amiR-ctrl*)	tttgtcttttatttcaggtcccagatctagggctctgcgtttgctccaggtagtccgctgctcccttgggcctgggcccactgacagc cctggtgcctctggccggctgcacacctcctggcgggcagctgtgttactgtaggatcgagagggatgttctggcaatacctgtc cctctccttactacagtaacacggaggcctgccctgactgcccacggtgccgtggccaaagaggatctaagggcaccgctgag ggcctacctaaccatcgtggggaataaggacagtgtcacccctgcaggggatccggtggtggtgcaaatca	
Human amiR-33-mouse shn3 (hs-*amiR-shn3*)	gatctggcagccttggagtgggttcctgccccctcgggcacacaaacagagctgaagaccaccctgggcacctccttggctgg ccgcatacctcctggcgggcagctgtgtacaaactacttgagagcaggtgttctggtggtacccacctgctctgtaatagtttgta cacagaggcctgcctggccctcgagagactgccctgactgaaggccctatcaggtgggggaggggatcctgatagagggca ctgctgccactgttggggcccaagctgca	
amiR-33-mouse shn3 (*amiR-shn3*)	tttgtcttttatttcaggtcccagatctagggctctgcgtttgctccaggtagtccgctgctcccttgggcctgggcccactgacagc cctggtgcctctggccggctgcacacctcctggcgggcagctgtgtacaaactacttgagagcaggtgttctggcaatacctgc ctgctctgtaatagtttgtacacggaggcctgccctgactgcccacggtgccgtggccaaagaggatctaagggcaccgctga gggcctacctaaccatcgtggggaataagg acagtgtcacccctgcaggggatccggtggtggtgcaaatca	
amiR-33-human shn3 (*amiR-hshn3*)	gtcttttatttcaggtcccagatcttagggctctgcgtttgctccaggtagtccgctgctcccttgggcctgggcccactgacagcc ctggtgcctctggccggctgcacacctcctggcgggcagctgtgtttccatggtaagttcaaggctgttctggcaatacctggcct tgaagatgccatggaaacacggaggcctgccctgactgcccacggtgccgtggccaaagaggatctaagggcaccgctgag ggcctacctaaccatcgtggggaataaggacagtgtcacccccctgcaggggatccggtggtggtgcaaat	
amiR-33-mouse sost (*amiR-sost*)	gatctagggctctgcgtttgctccaggtagtccgctgctcccttgggcctgggcccactgacagccctggtgcctctggccggct gcacacctcctggcgggcagctgtgtgacctctgtggcatcattcctgttctggcaatacctgggaatgatcgcgcagaggtcac acggaggcctgccctgactgcccacggtgccgtggccaaagaggatctaagggcaccgctgagggcctacctaaccatcgt ggggaataaggacagtgtcacccctgca	
amiR-33-mouse sost (*amiR-sost*) +	gatctagggctctgcgtttgctccaggtagtccgctgctcccttgggcctgggcccactgacagccctggtgcctctggccggct gcacacctcctggcgggcagctgtgtgacctctgtggcatcattcctgttctggcaatacctgggaatgatcgcgcagaggtcac	

human amiR-33 -mouse shn3 (hs-*amiR-shn3*)	acggaggcctgccctgactgcccacggtgccgtggccaaagaggatctaagggcaccgctgagggcctacctaaccatcgt ggggaataaggacagtgtcacccctgcaggggatccggtggtggtgcaaatcaaagaactgctcctcagtggatgttgccttta cttctaggcctgtacggaagtgttacttctgctctaaaagctgcggaattgtacccgcggccgatccaccggtcgccaccatggg gcagccttggagtgggttcctgccccctcgggcacacaaacagagctgaagaccaccctgggcacctccttggctggccgca tacctcctggcgggcagctgtgtacaaactacttgagagcaggtgttctggtggtacccacctgctctgtaatagtttgtacacag aggcctgcctggccctcgagagactgccctgactgaaggccctatcaggtgggggaggggatcctgatagagggcactgctg ccactgttggggcccaagaagct
Human amiR-33-human shn3-1 (hs-*amiR-hshn3-1*)	ggcagccttggagtgggttcctgccccctcgggcacacaaacagagctgaagaccaccctgggcacctccttggctggccgc atacctcctggcgggcagctgtgtttccatggtaagttcaaggctgttctggtggtacccagccttgaagatgccatggaaacac agaggcctgcctggccctcgagagactgccctgactgaaggccctatcaggtgggggaggggatcctgatagagggcactg ctgccactgttggggcccaag
Human amiR-33-human shn3-2 (hs-*amiR-hshn3-2*)	ggcagccttggagtgggttcctgccccctcgggcacacaaacagagctgaagaccaccctgggcacctccttggctggccgc atacctcctggcgggcagctgtgtccatggtaagttcaaggctgtgttctggtggtacccacagccttgttcctaccatggacaca gaggcctgcctggccctcgagagactgccctgactgaaggccctatcaggtgggggaggggatcctgatagagggcactgct gccactgttggggcccaag
Human SHN3 shR	ccgggccttgaacttaccatggaaactcgagtttccatggtaagttcaaggctttt